Journal of Magnetic Resonance 206 (2010) 274–279

Contents lists available at ScienceDirect

Journal of Magnetic Resonance

journal homepage: www.elsevier.com/locate/jmr

Communication

^{15}N–^{15}N spin–spin coupling constants through intermolecular hydrogen bonds in the solid state

Rosa M. Claramunt [a,*], Marta Pérez-Torralba [a], Dolores Santa María [a], Dionisia Sanz [a], Bénédicte Elena [b], Ibon Alkorta [c], José Elguero [c]

[a] Departamento de Química Orgánica y Bio-Orgánica, Facultad de Ciencias, UNED, Senda del Rey 9, E-28040 Madrid, Spain
[b] Université de Lyon, Centre de RMN à très hauts champs, CNRS/ENS Lyon/UCBL, 5 rue de la Doua, 69100 Villeurbanne, France
[c] Instituto de Química Médica (CSIC), Juan de la Cierva 3, E-28006 Madrid, Spain

ARTICLE INFO

Article history:
Received 18 May 2010
Revised 13 July 2010
Available online 30 July 2010

This paper is devoted to Professor José Manuel Concellón who untimely passed away.

Keywords:
Pyridine
Pyridinium
Hydrogen bond
J couplings
Solid-state NMR spectroscopy

ABSTRACT

A $^{2h}J_{NN}$ intermolecular spin–spin coupling constant (SSCC) of 10.2 ± 0.4 Hz has been measured for the powdered tetrachlorogallate salt of pyridinium solvated by pyridine (pyridine–$H^+\cdots$pyridine cation **3**). Density Functional Theory (DFT) calculations at the B3LYP/6-311++G(*d*, *p*) level reproduced this value and two others reported in the literature for ^{2h}J intermolecular SSCCs, which were measured for complexes in solution.

1. Introduction

Interest in the measurement of scalar NMR spin–spin coupling constants across hydrogen bonds is considerable due to their relevance for the structures of biomolecules. The experimental difficulty has limited most of these measurements, either in solution or in solids, to the 1/2 spin nuclei ^1H, ^{13}C, ^{15}N and ^{19}F, with few data involving ^{31}P; couplings with biologically interesting nuclei, such as ^{17}O, have been measured recently, for instance a $^{2h}J_{NO}$ has been measured in uracil [1]. To determine a coupling constant across a hydrogen bond (HB), several conditions must be fulfilled: (i) the HB strength must be moderate to high, which limits most studies to NH, OH and FH as HB donors and O(sp^2) and N(sp^2) as HB acceptors; and (ii) the geometry of the HB must be rigid. This latter requirement is not a problem if the HB is intramolecular, but if intermolecular this condition requires either biomolecules (nucleic acids, proteins) held together by multiple HBs or low-temperature studies. In the case of X–H$\cdots$Y complexes, the three constants $^1J_{XH}$, $^{1h}J_{HY}$ and $^{2h}J_{XY}$ can be measured if X and Y are 1/2 spin nuclei, but if one of the nuclei has a $I > 1/2$, for example, X = O and Y = N, then in general only one of the ^1J couplings, $^1J_{YH}$, can be determined (note the $^{2h}J_{NO}$ cited previously [1]).

In 1998, Dingley and Grzesiek [2] reported the first example of $^{2h}J_{NN}$, which refers to ^{15}N–^{15}N *J* couplings in solution. Using a uniformly $^{13}C/^{15}N$-enriched nucleotide, they measured averaged values of 6.7 ± 0.5 Hz for uracil/adenine and 6.3 ± 0.2 Hz for cytosine/guanine dimers. Concurrently, Pervushin et al. [3] described similar results for DNA, corresponding to 6.3 ± 0.3 Hz for cytosine/guanine and 6.8 ± 0.3 Hz for thymine/adenine. Other examples of biomolecules with observed coupling constants in this range have been reported [4] and we will cite only the case of the imidazolium/imidazole fragment in apomyoglobin, where a $^{2h}J_{NN}$ of 11.0 ± 1.0 Hz has been measured at pH = 4.9 [5].

In small molecules the $^{2h}J_{NN}$ couplings in solution, ranging from 16.5 Hz to 5.3 Hz, have primarily been determined for intramolecular hydrogen bonds [6,7]. The only contribution concerning intermolecular hydrogen bonds is due to Sijbesma et al. dealing with ureidopyrimidinones that exhibit $^{2h}J_{NN}$ couplings with values of about 5 Hz that, in some cases appeared to be temperature dependent [8].

A previously published report by Del Bene and Bartlett calculated a $^{2h}J_{NN}$ coupling for the CNH$\cdots$pyridine complex at 10.7 Hz, which was estimated from the Fermi contact term calculated with

* Corresponding author. Fax: +34 913988372.
E-mail address: rclaramunt@ccia.uned.es (R.M. Claramunt).

1090-7807/$ - see front matter © 2010 Elsevier Inc. All rights reserved.
doi:10.1016/j.jmr.2010.07.015

the EOM–CCSD approximation [9]. Analyses of these couplings at the SOPPA level for different N–H···N HBs, including anions and cations, have also been completed [10]. These results support the conclusion that $^{2h}J_{NN}$ depends on the hybridization of the hydrogen-bond donor N atom; $^{2h}J_{NN}$ does not depend on the hybridization of the hydrogen-bond acceptor N atom, and the dependence on the N atom hybridization is larger for charged complexes than for neutral ones.

In the following study, we focus on the measurement and calculation of $^{2h}J_{NN}$ in the solid state. Some of us [11,12] have previously reported intramolecular $^{2h}J_{NN}$ couplings in the 6-aminofulvene-1-aldimines at 7.3 ± 0.1 Hz and 8.0 ± 0.2 Hz, that are lower than those determined in solution [7]; this indicates that the intramolecular HBs are shorter in solution than in the solid state.

2. Results and discussion

2.1. $^{2h}J_{XY}$ spin–spin intermolecular coupling constants (SSCC)

The determination of spin–spin coupling constants across intermolecular HBs, $^{2h}J_{XY}$, in the solid state is particularly interesting because the crystal should prevent the dynamic characteristics present in solution even at low temperatures. Prior to this work, only three papers describe this type of coupling. In the first one, some of us reported a $^{2h}J_{NF}$ coupling of approximately 40 Hz in an organometallic complex **1** (Fig. 1a) [13], whose structure was previously solved (refcode UJOKEJ) [14,15]; in 2001 Limbach et al. determined that in solution, $^{2h}J_{NF}$ is equivalent to −96 Hz (F–H···collidine complex) [16], but this corresponds to a partial transfer of the proton to the base ($F^-\cdots H^+$–collidine).

Brown et al. described the measurement of $^{2h}J_{NN}$ in self-assembled guanosines by solid-state ^{15}N spin-echo MAS NMR [17]. In the guanosine trimeric ribbon **2** (Fig. 1b), for which the X-ray structure is known (refcode MOFBUE [15]), two intermolecular couplings were measured, however, only one smaller coupling was measured for the guanosine cyclic tetramer [18]. Finally, as aforementioned in the introduction a $^{2h}J_{NO}$ coupling for N–H···O intermolecular hydrogen bonds in uracil has been determined [1].

Theoretical calculations of $^{2h}J_{NN}$ couplings have been reported for intramolecular [19] and intermolecular situations [9,10]. In a subsequent paper, Joyce et al. [20] described DFT/CASTEP calculations of different N–H···N hydrogen bonded situations using a fully unconstrained geometry with fixed cell parameters, and their results were in excellent agreement to experimental data: fulvene-aldimines [11,12], exp. 7.3 ± 0.1 Hz, calcd. 7.4 Hz; exp. 8.0 ± 0.2 Hz calcd. 8.1 Hz; guanosine trimer **2** [17,18], exp. 7.4 ± 0.4 Hz, calcd. 7.7 Hz and exp. 6.2 ± 0.4 Hz, calcd. 6.5 Hz. In the experimental study, the N···N distances were 2.83 and 2.91 Å; however, in the theoretical paper, the N···N distances were 2.81 and 2.88 Å, which is an effect of relaxing the geometry.

2.2. Selection of a model for intermolecular SSCC measurement

We chose a complex presenting a strong N–H···N HB that possessed a geometry described in the CSD [15] and allowed accessible ^{15}N labeling strategies. The complex we selected was the pyridine–pyridinium tetrachlorogallate (**3**) (IKOHEV, Fig. 2) [21], as [^{15}N]-pyridine is commercially available. Complex **3** was prepared by exchanging [^{14}N]-pyridine with an excess of [^{15}N]-pyridine. ^{15}N CPMAS NMR data exhibited two signals at −157 ppm (NH^+) and −98 ppm (N) (*cf.* Section 4 for the detailed protocol).

2.3. ^{15}N CPMAS NMR experiments

The experimental *J* couplings were extracted from a series of 1D ^{15}N CP-MAS spin-echo experiments that were recorded for a sequence of spin-echo delay τ values, and the integrated intensities *S* in the frequency-domain spectra were fit to the following equation:

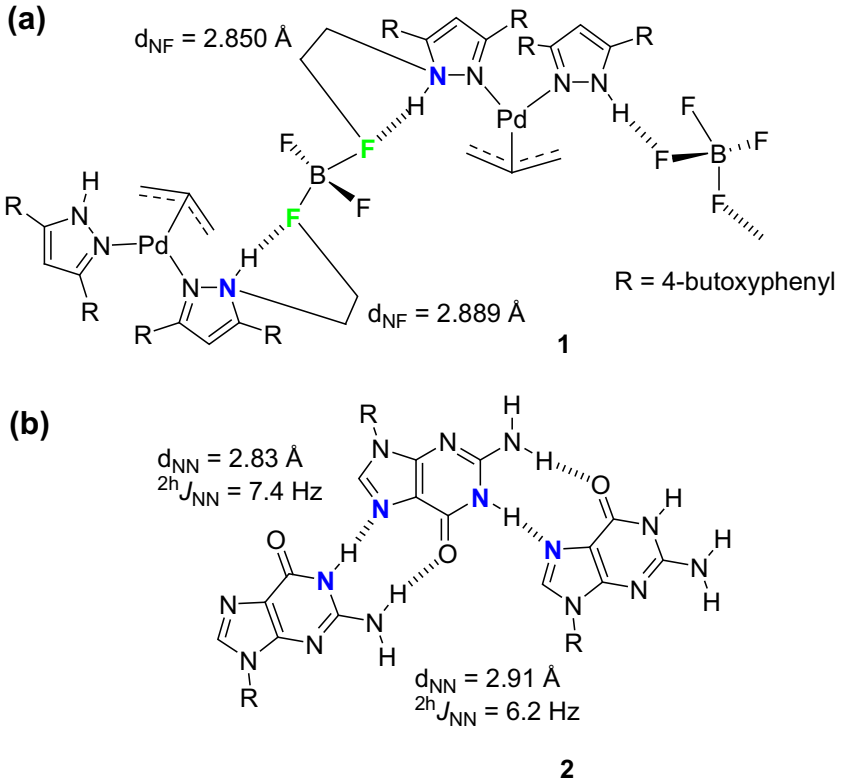

Fig. 1. Structures of: (a) the 3,5-di(4-butoxyphenyl)-1H-pyrazole Pd (II) complex tetrafluoroborate (**1**) and (b) the guanosine trimeric ribbon **2**.

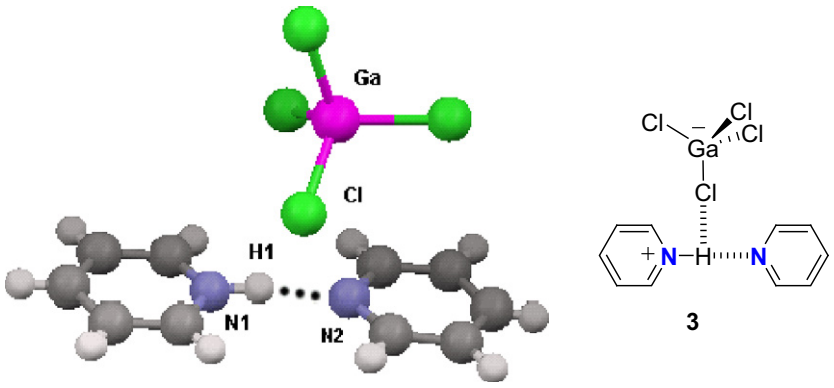

Fig. 2. The molecular structure of **3** [d_{N1N2} = 2.707 Å, d_{N1H1} = 0.946 Å, angle $N_1H_1N_2$ = 169(6)°].

$$S(\tau) = A\cos(2\pi J\tau)\exp(-2\tau/T_2')$$

In the plot of the experimental $S(\tau)$ against τ, the first zero crossing is observed at $\tau = 1/4J$ for N_1 and N_2 resonances (Fig. 3a), and $^{2h}J_{NN}$ values of 10.6 and 9.8 Hz, respectively, were derived with the average value calculated to be 10.2 ± 0.4 Hz.

The hydrogen-bond mediated J coupling, $^{2h}J(N_1–H\cdots N_2)$, was also identified using a two-dimensional ^{15}N refocused INADEQUATE [22] experiment; signals for both J-coupled nuclei were observed in this experiment (Fig. 3b).

2.4. SSCC theoretical calculations

The validity of our approach was evaluated by calculating (B3LYP/6-311++G(d, p) DFT method) the SSCC corresponding to the organometallic complex **1** [13] and the guanosine trimeric ribbon **2** [17,18] (Fig. 1). Our approach for calculating situations where the X-ray structure is known, was to use the experimental geometry for all non-hydrogen atoms and optimize all hydrogen atom positions. The resulting relaxed geometry is not a minimum, but the structure avoids the common problem of A–H distances from X-ray crystallography.

The study of $^{2h}J_{NF}$ SSCC in solution for intermolecular complexes is known to be particularly challenging. For example, the value of this coupling for the collidine/HF complex in solution (−96 Hz) [16] cannot be reproduced adequately even at the EOM/CCSD level (−57.0 Hz) [23]. Similarly, the coupling constant for the ammonia/HF complex (−43.7 Hz) is very sensitive to the geometry of the complex [24]. In solution, however, the proton should be partially transferred to the N atom (F···H^+–N) with concomitant shortening of the F···N distance and a large increase in the value of $^{2h}J_{NF}$. We have studied the reciprocal case of an N–H···F HB, but, in solution and for an intramolecular situation (2-fluorobenzamide) [25], the experimental value ($^{2h}J_{NF}$ = −7.3 Hz) was very well reproduced by the calculations (−7.4 Hz [B3LYP/6-311++G(d, p)]).

In this approach, the structure of the coordination complex **1** was simplified by removing the pyrazole substituents at positions 3 and 5, and only fragments with one or two pyrazoles were considered. The effect of coordination with a palladium/η^3-allyl complex was also evaluated. The results indicate that neither the complexation with palladium/η^3-allyl nor the second B–F···H–N HB modifies the SSCC appreciably; in contrast, the d_{NF} distance has a significant effect, and the largest coupling corresponded to the shortest distance. An average value of −25 Hz was calculated, which underestimates the experimental value of ∼|40| Hz; however, the experimental value includes a $^1J_{NH}$ of 8 Hz measured in solution that was not resolved in the ^{15}N CPMAS NMR spectrum, and a $^{2h}J_{NF}$ = |32| Hz is likely a better estimation.

In the guanosine trimeric ribbon **2**, the SSCC were calculated for the trimer and both possible dimers to determine possible cooperative (non-pairwise) effects (NPE). Clearly there are NPEs observed for the same N···N distance in which $^{2h}J_{NN}$ increases from 5.4 to 5.7 Hz and from 6.7 to 7.0 Hz. These values are lower than those determined experimentally at 6.2 and 7.4 Hz, but we have not allowed for a contraction of the HBs.

According to the theoretical calculations, complex **3** can adopt two structures; the perpendicular structure ($\mathbf{3}_{per}$, Table 1) is the minimum, and the planar one ($\mathbf{3}_{pla}$, Table 1), which exists only in the crystal, is a transition state. The results of the calculations are reported in Table 1 being consistent with the following conclusions: (i) The difference in conformation (perpendicular vs. planar, entries 1 and 2) has a small effect on $^{2h}J_{NN}$; the perpendicular geometry corresponds to the minimum, which has a shorter distance d_{NN} and consequently a larger SSCC (14.1 vs. 13.6 Hz); however, when d_{NN} is fixed (entries 3 and 4, d_{NN} = 2.707 Å), the planar conformation has the larger SSCC (14.0 vs. 13.6 Hz). (ii) The tetrachlorogallate anion has a small effect on the SSCC (entries 5 and 6); when all other variables are held constant, the anion decreases $^{2h}J_{NN}$ by 0.3 Hz. (iii) Calculations that include the $GaCl_4^-$ anion (entries 5, 7 and 8) show the effect of the geometry on the HB: a total optimization leads to d_{NN} = 2.740 Å, d_{NH} = 1.090 Å and $^{2h}J_{NN}$ = 12.6 Hz. When setting d_{NH} according to the X-ray determined proton position (d_{NH} = 0.946 Å), the $^{2h}J_{NN}$ coupling decreases to 9.3 Hz; removal of this constraint (entry 8) results in an increase of the $^{2h}J_{NN}$ coupling to 13.7 Hz. The actual position of the NH (NH bond length and NHN bond angle) should be intermediate between that determined by X-ray crystallography (a well-known problem resulting in abnormally short X–H distances) [26] and the one calculated for the gas phase. As studied for **3**, the effect of anions on the $^{2h}J_{NN}$ present in proton sponges has been examined by Limbach et al. [6]. Strong coordination of the anion with the proton of the HB was found to weaken the HB, which becomes more asymmetric, and $^{2h}J_{NN}$ decreases; in contrast, anions that are less solvating will increase the observed coupling. In our case, the small decrease should be related to the $Cl_3GaCl\cdots H^+$ interaction.

A plot of the $^{2h}J_{NN}$ values calculated in this work for compounds **2** and **3** against the N···N distance is presented in Fig. 4; a compilation of $^{2h}J_{NN}$ couplings calculated at the B3LYP/6-311++G(d, p) level for a great variety of N–H···N HBs is also shown [10]. Clearly, the results from this study are in agreement with those previously calculated. According to the trendline, in compound **2**, the shortening of the N···N distances from 2.83 to 2.81 and from 2.91 to 2.88 Å [20] increases $^{2h}J_{NN}$ by 1.07 and 1.11 Hz, respectively. Thus, for these shorter HBs, the couplings should be 7.5 and 6.3 Hz, which are very close to the experimental values of 7.4 and 6.2 Hz [17,18]. This strongly indicates that the calculation method is less important than consideration of the geometry of the HBs [10].

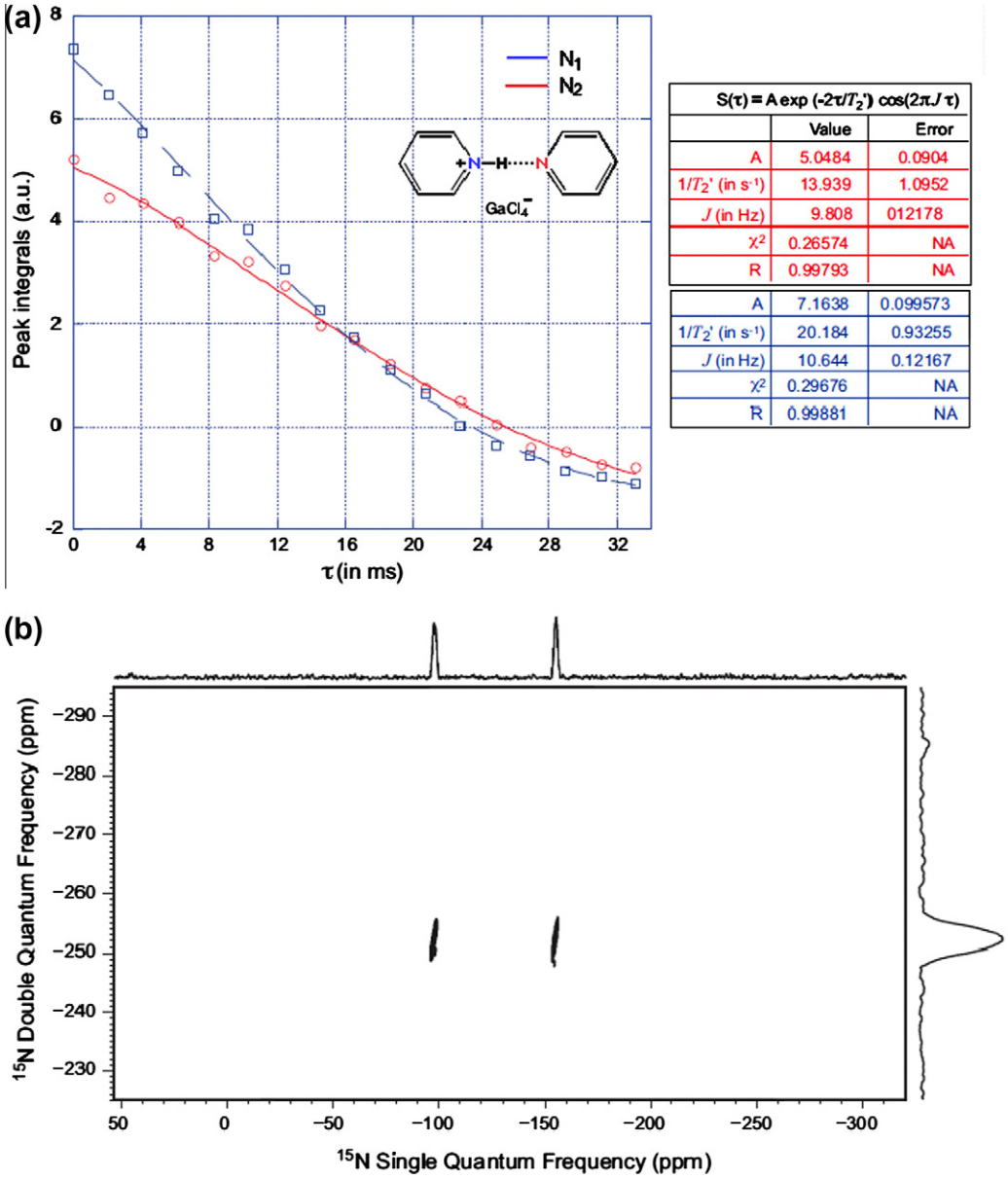

Fig. 3. (a) Experimental determination of $^{2h}J_{NN}$ in complex **3**. (b) 2D ^{15}N refocused-INADEQUATE solid-state NMR spectrum of **3** recorded at 700 MHz (^{1}H resonance frequency).

3. Conclusions

The first example of an intermolecular $^{2h}J_{NN}$ in the solid state for a cationic species, the tetrachlorogallate salt of pyridinium/pyridine (**3**) has been determined, both experimentally and via DFT calculations. The value for this ^{15}N–^{15}N *J* coupling through an intermolecular hydrogen bond, 10.2 Hz, is similar to those measured in solution for the imidazolium/imidazole fragment in apomyoglobin (11.0 Hz [5]) and for some protonated proton sponges (9.9 Hz [6]).

4. Experimental

4.1. Pyridine–pyridinium tetrachlorogallate (**3**) [Py···H–Py][$GaCl_4$]

A solution of pyridinium chloride (1.32 g, 11.42 mmol) in 30 mL of dry pyridine was added to a solution of $(GaCl_3)_2$ (2.0 g, 11.36 mmol) in 10 mL of dry pyridine. The reaction was stirred for 1 h at room temperature under an argon atmosphere. The excess pyridine was evaporated, and the residue was crystallized from toluene to yield pyridine–pyridinium tetrachlorogallate (III) (**3**) (4.0 g, 95%). M.p. (SEIKO DSC 220C, scanning rate: 5.0 °C per min, sample size 0.004 g) 98.7 °C (lit. 116 °C) [21]; ^{1}H NMR (400.13 MHz, DMSO-d_6): δ = 8.75 (*d*, $^{3}J_{H2/H6-H3/H5}$ = 4.7 Hz, H-2/H-6), 8.22 (dddd, $^{3}J_{H4-H3} = {}^{3}J_{H4-H5}$ = 7.7 Hz, $^{4}J_{H4-H2} = {}^{4}J_{H4-H6}$ = 1.7 Hz, H-4), 7.75 (m, H-3/H-5); ^{13}C NMR (100.62 MHz, DMSO-d_6) δ = 145.5 (C-2/C-6), 141.6 (C-4), 125.7 (C-3/C-5); elemental analysis calcd. (%) for $C_{10}H_{11}N_2GaCl_4$ (370.74): C 32.40, H 2.99, N 7.56; found: C 32.03, H 3.01, N 7.50.

4.2. Pyridine–pyridinium tetrachlorogallate (**3**) [Py···H–Py][$GaCl_4$] [^{15}N]-labeled

One hundred and four milligram of unlabeled pyridine–pyridinium tetrachlorogallate (**3**) was dissolved in 150 μL of [^{15}N]-labeled pyridine. The mixture was allowed to stand for 17 h under an argon atmosphere at room temperature, and then the excess

Table 1
Theoretical calculations of $^{2h}J_{NN}$ in Hz for complex **3**

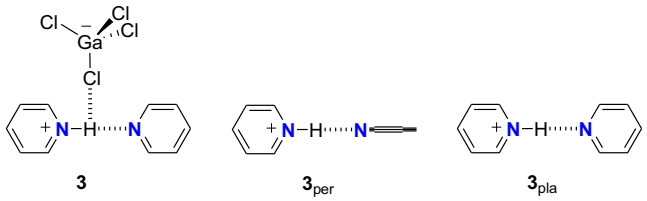

3 **3_{per}** **3_{pla}**

Entry	Conformation	Anion	Geometry constrains	d_{NN} (Å)	d_{NH} (Å)	HNH (°)	Code	$^{2h}J_{NN}$
1	Perpendicular	None	None	2.687	1.107	180.0[a]	$\mathbf{3}_{per}$	14.1[b]
2	Planar	None	None	2.722	1.097	180.0[a]	$\mathbf{3}_{pla}$	13.6
3	Perpendicular	None	d_{NN} fixed	2.707[c]	1.103	180.0[a]	$\mathbf{3}_{per}$	13.6
4	Planar	None	d_{NN} fixed	2.707[c]	1.102	180.0[a]	$\mathbf{3}_{pla}$	14.0
5	Planar	$GaCl_4^-$	None	2.740	1.090	178.0	**3**	12.6
6	Planar	None	Identical to entry 5	2.740	1.090	178.0	$\mathbf{3}_{pla}$	12.9
7	Planar	$GaCl_4^-$	Only CH optimized	2.707[c]	0.946	166.9	**3**	9.3
8	Planar	$GaCl_4^-$	All H optimized	2.707[c]	1.107	175.7	**3**	13.7
9	Planar	None	Experimental data	2.707[c]	0.946	169.0	$\mathbf{3}_{pla}$	10.0
Exp.	Planar	$GaCl_4^-$	–	2.707	0.946	169(6)	**3**	10.2 ± 0.4

[a] C_{2v}.
[b] A SOPPA calculation lead to a $^{2h}J_{NN}$ = 15.5 Hz.
[c] Experimental.

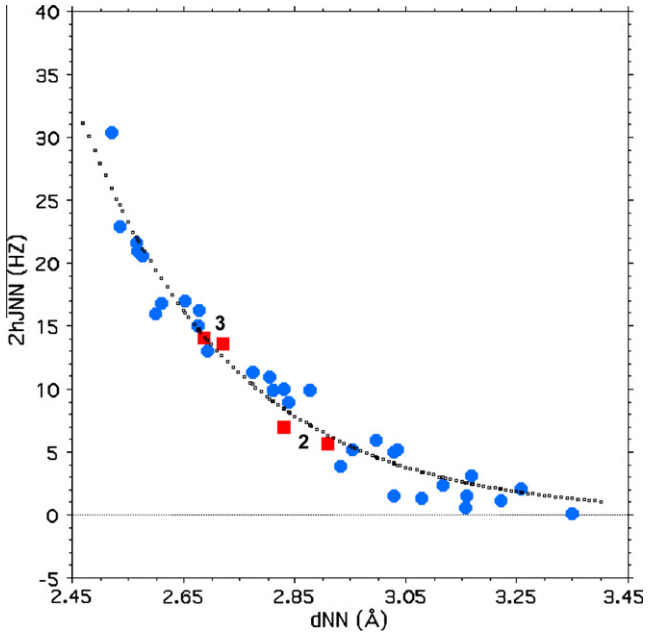

Fig. 4. Scatter of $^{2h}J_{NN}$ coupling constants vs. N···N distances for compounds **2** and **3**. Blue points: from Ref. [10]; red squares: this work; trendline: $^{2h}J_{NN} = 240{,}795 * e^{(-3.624*dNN)}$, $R^2 = 0.953$. (For interpretation of the references to color in this figure legend, the reader is referred to the web version of this article.)

solvent was removed. The residue is ^{15}N-labeled **3** (isotope abundance approximately 70% by NMR integration of C-4 signals). ^{1}H NMR (400.13 MHz, THF-d_8): δ = 8.76 (dd, $^3J_{H2/H6-H3/H5} = {}^2J_{H2N/H6N}$ = 5.5 Hz, H-2/H-6), 8.23 (dd, $^3J_{H4-H3} = {}^3J_{H4-H5}$ = 7.7 Hz, H-4), 7.78 (m, H-3/H-5) ppm; ^{13}C NMR (100.62 MHz, THF-d_8): δ = 146.71 (C-2/C-6), 146.65 ($^1J_{CN}$ = 5.0, C-2/C-6), 142.97 ($^3J_{CN}$ = 4.1, C-4), 142.90 (C-4), 126.91 (C-3/C-5) ppm; ^{15}N NMR (40.56 MHz, THF-d_8): δ = −126.9 ppm.

4.3. NMR Studies

Solution NMR spectra were recorded at 300 K on a Bruker DRX 400 (9.4 Tesla, 400.13 MHz for ^{1}H, 100.62 MHz for ^{13}C and 40.56 MHz for ^{15}N) spectrometer with a 5-mm inverse-detection H-X probe equipped with a *z*-gradient coil. Chemical shifts (δ in ppm) are given from internal solvent references: $CDCl_3$, 7.26 for ^{1}H and 77.0 for ^{13}C; THF-d_8, 3.58 for ^{1}H and 67.6 for ^{13}C. Typical parameters for ^{1}H NMR spectra included a spectral width of 5500 Hz, a pulse width of 7.5 μs and a resolution of 0.33 Hz per point. Typical parameters for ^{13}C NMR spectra included a spectral width of 20,600 Hz, a pulse width of 10.6 μs and a resolution of 0.63 Hz per point; WALTZ-16 was used for broadband proton decoupling, and the FIDS were multiplied by an exponential weighting (*lb* = 1 Hz) before Fourier transformation.

Solid-state experiments were conducted on a Bruker Avance II spectrometer operating at 700 MHz (^{1}H resonance frequency) and using a 3.2 mm triple resonance probe. The temperature was regulated at 295 K, and the magic angle spinning frequency was set to 22,222 Hz. ^{15}N transverse magnetization was obtained using ramped cross-polarization from ^{1}H with a contact time of 5 ms, and proton heteronuclear dipolar decoupling was achieved using the SPINAL-64 scheme and a decoupling field strength of 100 kHz. The recycle delay was set to 15 s. In the CP-MAS spin-echo experiment, the rotor-synchronized delay τ was varied in the range [0; 33.12 ms]. In the 2D refocused INADEQUATE experiment, a 141 ppm sweep width was used in the indirect dimension of acquisition, and 64 transients were co-added for each of the 64 t_1 points. The rotor-synchronized evolution time τ was set to 9.99 ms. ^{15}N spectra were originally referenced to $^{15}NH_4Cl$, and the spectra were then converted to the nitromethane scale using the relationship: δ^{15}N(nitromethane) = δ^{15}N(ammonium chloride) − 338.1 ppm.

4.4. Computational details

The geometries of the systems have been fully optimized at the B3LYP/6-311++G** level with the Gaussian 03 facilities [27]. Frequency calculations have been carried out to confirm that the fully optimized structures correspond to energy minima. Coupling constants were calculated at the B3LYP/6-311++G** level and, in one case, at the SOPPA level [28].

Acknowledgments

The authors are grateful to Professor Lyndon Emsley for his scientific help. Thanks are also given to the Ministerio de Ciencia e

Innovación (Projects CTQ2007-61901/BQU and CTQ2007-62113) and Comunidad Autónoma de Madrid (Project MADRISOLAR, S-0505/PPQ/0225) for financial help. Economic support by the Access to Research Infrastructures activity in the 6th Framework Program of the EC (Contract # RII3-026145, EU-NMR) for conducting this research is acknowledged.

References

[1] I. Hung, A.-C. Uldry, J. Becker-Baldus, A.L. Webber, A. Wong, M.E. Smith, S.A. Joyce, J.R. Yates, C.J. Pickard, R. Dupree, S.P. Brown, Probing heteronuclear ^{15}N–^{17}O and ^{13}C–^{17}O connectivities and proximities by solid-state NMR spectroscopy, J. Am. Chem. Soc. 131 (2009) 1820–1834.

[2] A.J. Dingley, S. Grzesiek, Direct observation of hydrogen bonds in nucleic acid base pairs by internucleotide $^{2}J_{NN}$ couplings, J. Am. Chem. Soc. 120 (1998) 8293–8297.

[3] K. Pervushin, A. Ono, C. Fernández, T. Szyperski, M. Kainosho, K. Wüthrich, NMR scalar couplings across Watson–Crick base pair hydrogen bonds in DNA observed by transverse relaxation-optimized spectroscopy, Proc. Natl. Acad. Sci. 95 (1998) 14147–14151.

[4] I. Alkorta, J. Elguero, G.S. Denisov, A review with comprehensive data on experimental indirect scalar NMR spin–spin coupling constants across hydrogen bonds, Magn. Reson. Chem. 45 (2008) 599–624.

[5] M. Hennig, B. Geierstanger, Direct detection of a histidine–histidine side chain hydrogen bond important for folding of apomyoglobin, J. Am. Chem. Soc. 121 (1999) 5123–5126.

[6] M. Pietrzak, J.P. Wehling, S. Kong, P.M. Tolstoy, I.G. Shenderovich, C. López, R.M. Claramunt, J. Elguero, G.S. Denisov, H.-H. Limbach, Symmetrization of cationic hydrogen bridges of protonated sponges induced by solvent and counteranion interactions as revealed by NMR spectroscopy, Chem. – Eur. J. 16 (2010) 1679–1690.

[7] R.M. Claramunt, D. Sanz, S.H. Alarcón, M. Pérez Torralba, J. Elgero, C. Foces-Foces, M. Pietrzak, U. Langer, H.-H. Limbach, 6-Aminofulvene-1-aldimine: a model molecule for the study of intramolecular hydrogen bonds, Angew. Chem., Int. Ed. 40 (2001) 420–423.

[8] S.H. Söntjens, M.H.P. van Gerderen, R.P. Sijbesma, Intermolecular $^{2h}J_{NN}$ coupling in multiply hydrogen-bonded ureidopyrimidinone dimers in solution, J. Org. Chem. 68 (2003) 9070–9075.

[9] J.E. Del Bene, R.J. Bartlett, N–N spin–spin coupling constants [$^{2h}J(^{15}N–^{15}N)$] across N–H···N hydrogen bonds in neutral complexes: to what extent does the bonding at the nitrogens influence $^{2h}J_{N–N}$?, J Am. Chem. Soc. 122 (2000) 10480–10481.

[10] I. Alkorta, F. Blanco, J. Elguero, A theoretical structural analysis of the factors that affect $^{1}J_{NH}$, $^{1h}J_{NH}$ and $^{2h}J_{NN}$ in N–H···N hydrogen-bonded complexes, Magn. Reson. Chem. 47 (2009) 249–256.

[11] S.P. Brown, M. Pérez Torralba, D. Sanz, R.M. Claramunt, L. Emsley, the direct detection of a hydrogen bond in the solid state by NMR through the observation of a hydrogen-bond mediated ^{15}N–^{15}N *J* coupling, J. Am. Chem. Soc. 124 (2002) 1152–1153.

[12] S.P. Brown, M. Pérez Torralba, D. Sanz, R.M. Claramunt, L. Emsley, Determining hydrogen-bond strengths in the solid state by NMR: the quantitative measurement of ^{15}N–^{15}N *J* couplings, Chem. Commun. (2002) 1852–1853.

[13] P. Cornago, R.M. Claramunt, M. Cano, J.V. Heras, M.L. Gallego, Multinuclear NMR study of Au(I), Pd(II) and Ag(I) pyrazole complexes to investigate the coordination mode, Arkivoc ix (2005) 21–29.

[14] R.M. Claramunt, P. Cornago, M. Cano, J.V. Heras, M.L. Gallego, E. Pinilla, M.R. Torres, New tris(pyrazolyl)triazine pyrazolylpyridine gold(I) palladium(II) derivatives based on the 3,5-bis(4-butoxyphenyl)pyrazole group architectures with different types of bonding interactions, Eur. J. Inorg. Chem. (2003) 2693–2704.

[15] F.H. Allen, The Cambridge structural database: a quarter of a million crystal structures and rising, Acta Crystallogr., Sect. B B58 (2002) 380–388;
F.H. Allen, W.D.S. Motherwell, Applications of the Cambridge structural database in organic chemistry and crystal chemistry, Acta Crystallogr., Sect. B B58 (2002) 407–422 (CSD version 5.30 (updates February 2009)).

[16] I.G. Shenderovich, A.P. Burtsev, G.S. Denisov, N.S. Golubev, H.-H. Limbach, Influence of the temperature-dependent dielectric constant on the H/D isotope effects on the NMR chemical shifts and the hydrogen bond geometry of the collidine–HF complex in $CDF_3/CDClF_2$ solution, Magn. Reson. Chem. 39 (2001) S91–S99.

[17] T.N. Pham, J.M. Griffin, S. Masiero, S. Lena, G. Gottarelli, P. Hodkinson, C. Filip, S.P. Brown, Quantifying hydrogen-bonding strength: the measurement of $^{2h}J_{NN}$ couplings in self-assembled guanosines by solid-state ^{15}N spin-echo MAS NMR, Phys. Chem. Chem. Phys. 9 (2007) 3416–3423.

[18] T.N. Pham, S. Masiero, G. Gottarelli, S.P. Brown, Identification by ^{15}N refocused INADEQUATE MAS NMR of intermolecular hydrogen bonding that directs the self-assembly of modified DNA bases, J. Am. Chem. Soc. 127 (2005) 16018–16019.

[19] I. Alkorta, J. Elguero, O. Mó, M. Yáñez, J.E. Del Bene, Are resonance-assisted hydrogen bonds 'resonance assisted'? A theoretical NMR study, Chem. Phys. Lett. 411 (2005) 411–415.

[20] S.A. Joyce, J.R. Yates, C.J. Pickard, S.P. Brown, Density functional theory calculations of hydrogen-bond-mediated NMR *J* coupling in the solid state, J. Am. Chem. Soc. 130 (2008) 12663–12670.

[21] S. Nogai, A. Schriewer, H. Schmidbaur, Reactions of trichlorogermane $HGeCl_3$ and dichlorogallane $HGaCl_2$ with pyridine donors, Dalton Trans. (2003) 3165–3171.

[22] A. Lesage, M. Bardet, L. Emsley, Through-bond carbon–carbon connectivities in disordered solids by NMR, J. Am. Chem. Soc. 121 (1999) 10987–10993.

[23] J.E. Del Bene, J. Elguero, Predicted signs of reduced two-bond spin–spin coupling constants ($^{2h}K_{X–Y}$) across X–H–Y hydrogen bonds, Magn. Reson. Chem. 42 (2004) 421–423.

[24] J.E. Del Bene, R.J. Bartlett, J. Elguero, Interpreting ^{2h}J(F, N), ^{1h}J(H, N) and ^{1}J(F, H) in the hydrogen-bonded FH–collidine complex, Magn. Reson. Chem. 40 (2002) 767–771.

[25] I. Alkorta, J. Elguero, H.-H. Limbach, I.G. Shenderovich, T. Winkler, A DFT and AIM analysis of the spin–spin couplings across the hydrogen bond in the 2-fluorobenzamide and related compounds, Magn. Reson. Chem. 47 (2009) 585–592.

[26] J. Almlöf, T. Ottersen, X-ray high-order refinements of hydrogen atoms: a theoretical approach, Acta Crystallogr., Sect. A A35 (1979) 137–139.

[27] M.J. Frisch, G.W. Trucks, H.B. Schlegel, G.E. Scuseria, M.A. Robb, J.R. Cheeseman, J.A. Montgomery Jr., T. Vreven, K.N. Kudin, J.C. Burant, J.M. Millam, S.S. Iyengar, J. Tomasi, V. Barone, B. Mennucci, M. Cossi, G. Scalmani, N. Rega, G.A. Petersson, H. Nakatsuji, M. Hada, M. Ehara, K. Toyota, R. Fukuda, J. Hasegawa, M. Ishida, T. Nakajima, Y. Honda, O. Kitao, H. Nakai, M. Klene, X. Li, J.E. Knox, H.P. Hratchian, J.B. Cross, C. Adamo, J. Jaramillo, R. Gomperts, R.E. Stratmann, O. Yazyev, A.J. Austin, R. Cammi, C. Pomelli, J.W. Ochterski, P.Y. Ayala, K. Morokuma, G.A. Voth, P. Salvador, J.J. Dannenberg, V.G. Zakrzewski, S. Dapprich, A.D. Daniels, M.C. Strain, O. Farkas, D.K. Malick, A.D. Rabuck, K. Raghavachari, J.B. Foresman, J.V. Ortiz, Q. Cui, A.G. Baboul, S. Clifford, J. Cioslowski, B.B. Stefanov, G. Liu, A. Liashenko, P. Piskorz, I. Komaromi, R.L. Martin, D.J. Fox, T. Keith, M.A. Al-Laham, C.Y. Peng, A. Nanayakkara, M. Challacombe, P.M.W. Gill, B. Johnson, W. Chen, M.W. Wong, C. Gonzalez, J.A. Pople, Gaussian 03, Gaussian, Inc., Pittsburgh PA, 2003.

[28] (a) E.S. Nielsen, P. Jørgensen, J. Oddershede, Transition moments and dynamic polarizabilities in a second order propagator approach, J. Chem. Phys. 73 (1980) 6238–6246;
(b) M.J. Packer, E.K. Dalskov, T. Enevoldsen, H.J.A. Jensen, J. Oddershede, A new implementation of the second-order polarization propagator approximation (SOPPA): the excitation spectra of benzene and naphthalene, J. Chem. Phys. 105 (1996) 5886–5900;
(c) J. Geertsen, J. Oddershede, Second-order polarization propagator calculations of indirect nuclear spin–spin coupling tensors in the water molecule, Chem. Phys. 90 (1984) 301–311.